Supporting Information

Structural Correspondence of the Oriented Attachment Growth Mechanism of Crystals of the Pharmaceutical Dirithromycin

Zuozhong Liang,[†] *Yuan Wang,*[†] *Wei Wang,*[†] *Xianglong Han,*[†] *Jian-Feng Chen,*[*,†,‡]

Chunyu Xue,[*,§] *Hong Zhao*[*,†]

[†] *State Key Laboratory of Organic-Inorganic Composites, Beijing University of Chemical Technology, Beijing 100029, China*

[‡] *Research Center of the Ministry of Education for High Gravity Engineering and Technology, Beijing University of Chemical Technology, Beijing 100029, China*

[§] *Biomass Energy and Environmental Engineering Research Center, Beijing University of Chemical Technology, Beijing 100029, China*

Corresponding authors:

Email:chenjf@mail.buct.edu.cn; Tel: +86-10-64446466;

E-mail:xuecy@mail.buct.edu.cn; Tel: +86-10-64442375;

E-mail:zhaohong @mail.buct.edu.cn.; Tel.:+86-10-64433134;

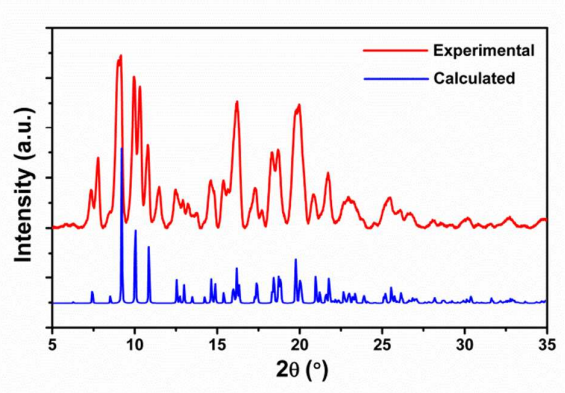

Figure S1. Experimental and calculated (Form II) X-ray diffraction patterns of DIR raw materials.

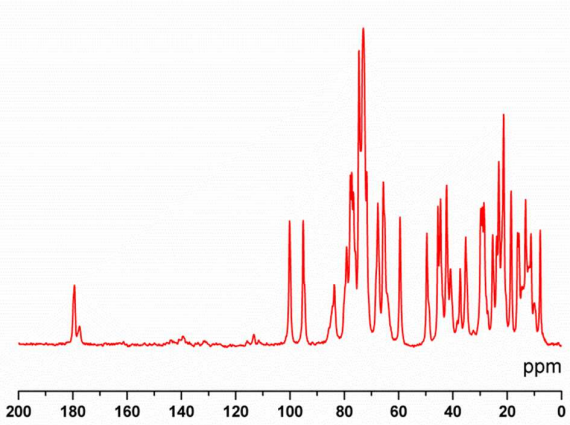

Figure S2. ^{13}C solid-state NMR spectrum of the raw material DIR.

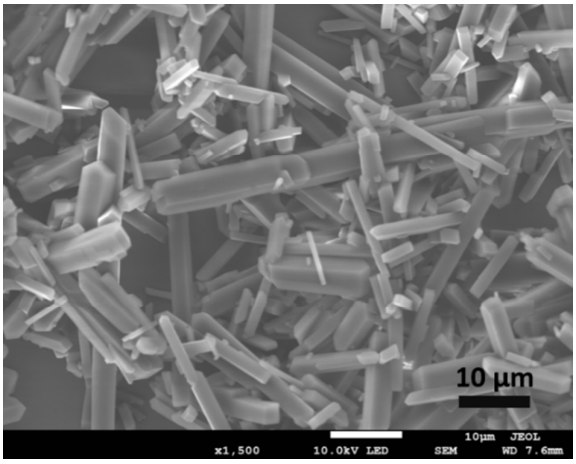

Figure S3. SEM image of the precursors of DIR crystals in DMF solvent.

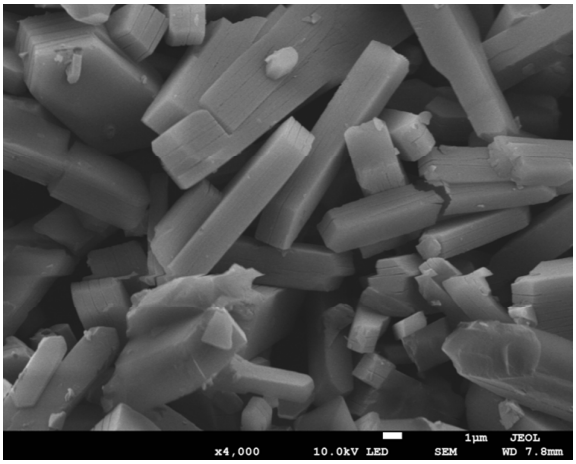

Figure S4. SEM characterization of the DIR in DMF solvent by solvothermal method at 40 °C for 24h.

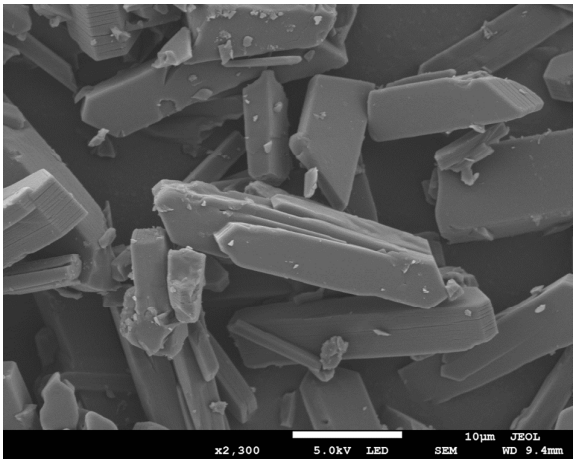

Figure S5. SEM characterization of the DIR in DMF solvent by solvothermal method at 40 °C for 48h.

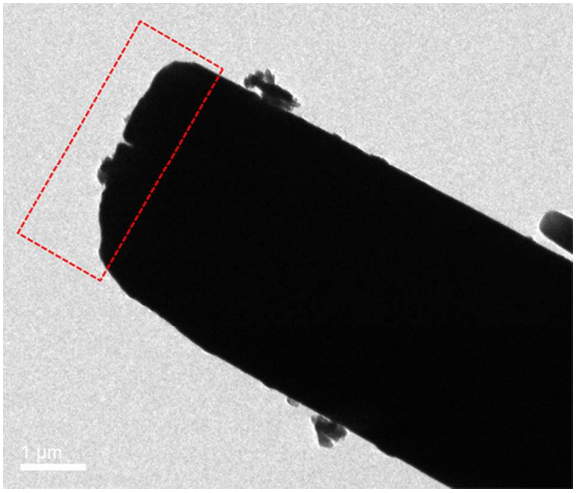

Figure S6. TEM image of DIR crystals in DMF solvent by solvothermal treatment at 40 °C for 48h.

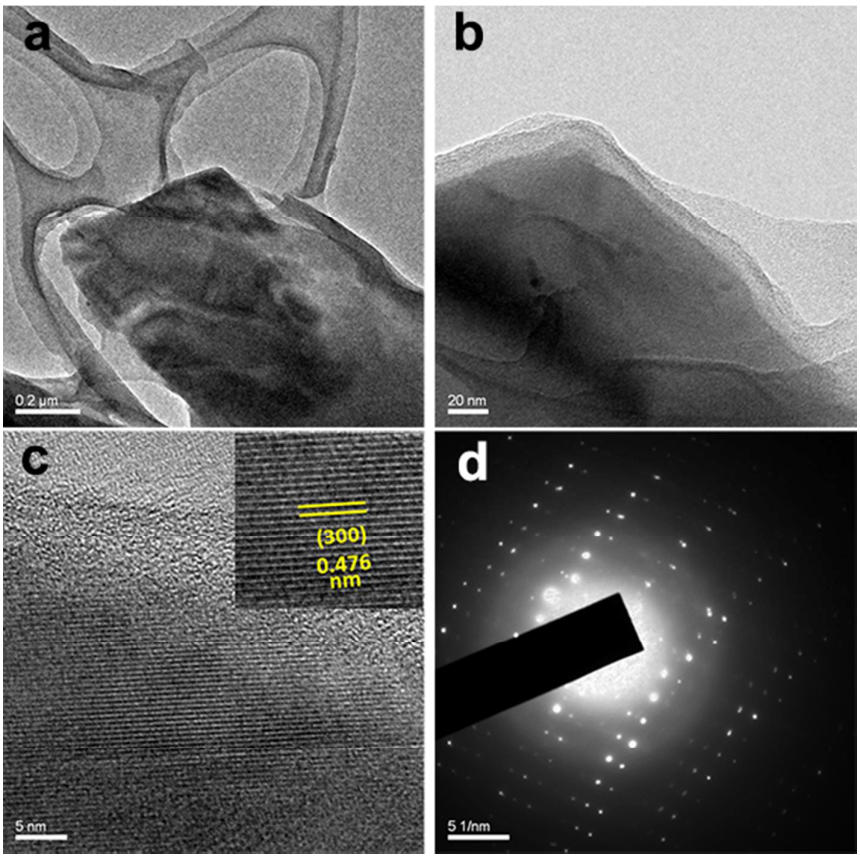

Figure S7. TEM images (a & b), high-resolution TEM (HRTEM) image (c), and their SAED pattern (d) of solvothermal synthesized DIR crystals at 40 °C for 48h.

Table S1. E_{surf}(Total), E_{surf}(vdW), E_{surf}(Electrostatic)(J/m^2), and total surface areas (%) for equilibrium morphology of DIR.

Face	E_{surf}(Total)	E_{surf}(vdW)	E_{surf}(Electrostatic)	Area
(001)	0.151	0.136	0.015	18.56%
(100)	0.158	0.156	0.002	7.74%
(10−1)	0.156	0.145	0.010	3.27%
(101)	0.204	0.193	0.011	0.38%

(011)	0.175	0.165	0.010	1.39%
(0−11)	0.175	0.165	0.010	1.39%
(110)	0.136	0.134	0.002	16.05%
(1−10)	0.136	0.134	0.002	16.05%
(11−1)	0.142	0.135	0.007	10.35%
(1−1−1)	0.142	0.135	0.007	10.35%
(111)	0.179	0.168	0.01	1.66%
(1−11)	0.179	0.168	0.01	1.66%

Table S2. The *a, b,* and *c* (Å) of the modelling box and area values (A_{hkl} and A_{box}; Å^2) for main exposed faces of DIR growth morphology.

Faces	*a*	*b*	*c*	A_{hkl}	A_{box}
(001)	43.11	35.09	89.87	1512.73	17081
(100)	35.09	44.09	89.54	1547.00	17273
(10−1)	35.09	58.98	90.97	2069.61	21254
(011)	43.12	56.34	92.73	2429.38	23304
(0−11)	43.12	56.34	94.11	2429.38	23579
(110)	44.09	55.59	84.34	2450.96	23716
(1−10)	55.59	44.09	86.14	2450.96	22074

Table S3. The area values (A_{acc} and A_{hkl}; Å^2) and correction factor *S* (S=A_{acc}/A_{hkl}) of 3D supercells of three cleaved surfaces including (001), (100) and (110) with dimensions $2a \times 2b \times 3c$. Here, the A_{acc} indicates the accessible solvent surface and the A_{hkl} stands for the top surface area ($2a \times 2b$) of a supercell.

Faces	A_{acc}	A_{hkl}	*S*
(001)	832.11	672.36	1.238
(100)	924.24	687.48	1.344
(110)	1323.92	1089.16	1.216

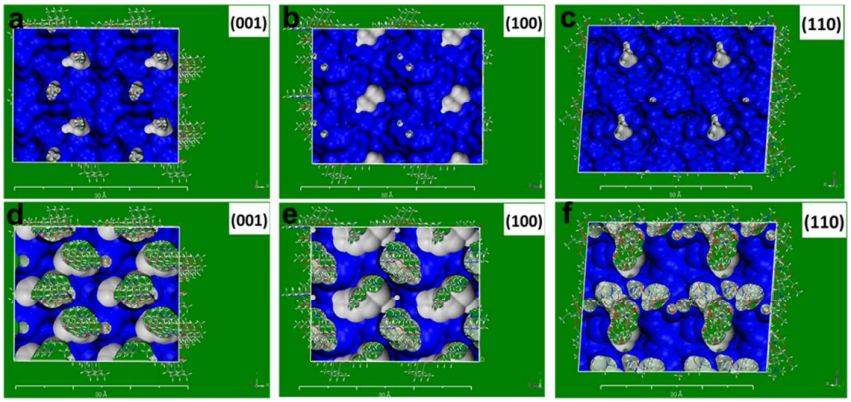

Figure S8. Connolly surfaces (a, b, and c) and accessible solvent surfaces (d, e, and f) of three crystal faces (001), (100) and (110).

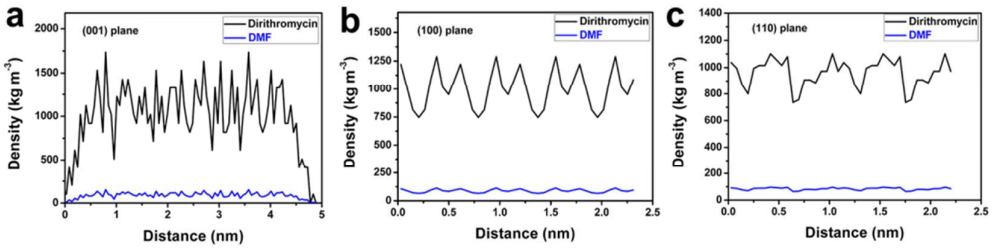

Figure S9. Density profiles for crystalline DIR at the (001) plane (a), (100) plane (b), and (110) plane (c) as a function of distance.

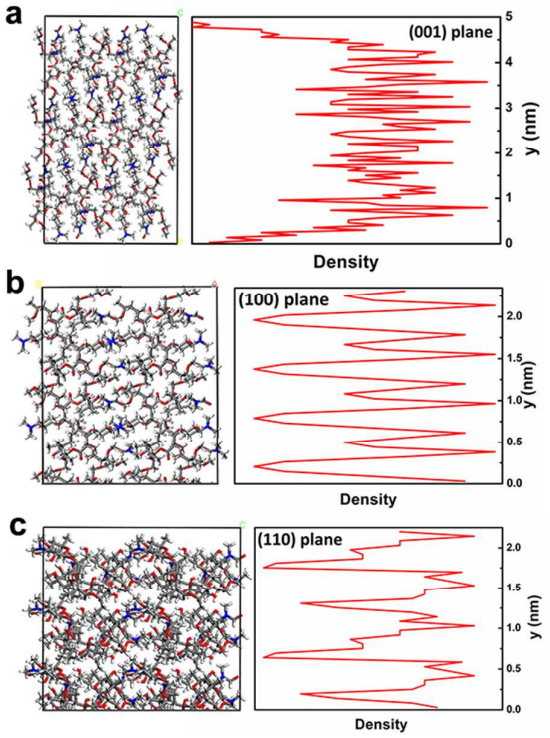

Figure S10. Visual illustration of the interfacial distribution of compounds along with the density profiles side by side at three planes (001), (100), and (110).

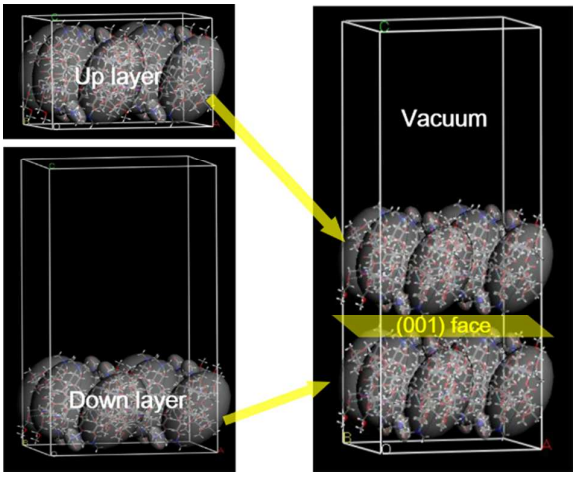

Figure S11. Diagram showing the oriented attachment (OA) computational model in which two cleaved supercells (up and down layer) are attached facet-to-facet on the surface (001). The ellipse displays the configuration of DMF and DIR molecule.

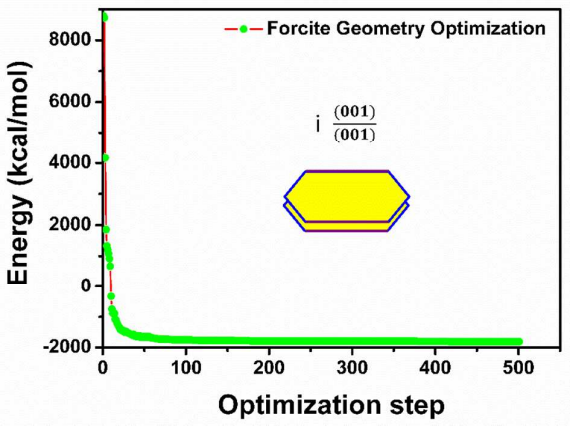

Figure S12. The $E_{attached}$ of OA configuration i during Forcite Geometry Optimization.